SUPPLEMENTARY MATERIAL for

Aqueous secondary organic aerosol formation in ambient cloud water photo-oxidations

M.I. Schurman[1,2*], A. Boris[1], Y. Desyaterik[1], J. L. Collett, Jr. [1]

S1: AMS Calibrations, Data Quality, Collection Efficiency, and Other Information

AMS data quality is enhanced by initial mass spectrometer tuning, aerodynamic lens alignment, and calibrations pertinent to electron multiplier gain, flow rate, and particle sizing (in this case particle size is a function of atomizer output, so the sizing mode was not used), with subsequent ionization efficiency calibrations (≥2 times per week); quality assurance during sampling includes periodic HEPA filtration (to verify inlet integrity, etc.), atomization of deionized water (18 microOhm conductivity) to check for aqueous system contamination, mass spectrometer *m/z* calibrations, chopper position checks, ancillary data collection, and logs chronicling instrument function. Final calibrations include ionization efficiency, flow rate, and particle size to evaluate instrument drift over the course of the experiment.

AMS Function and CE

AMS instrument details for TaiOx laboratory campaign

AMS_Type: HR: V and W

AMS_SamplingTime: 1 minute runs: V mode (10 sec ea open and closed, 20sec PToF, 3cycles/run) and W mode (20 sec ea open and closed, 3cycles/run)

AMS_LensType: standard

AMS_FlowRate: study average=1.47 ± 0.02 cm^3/sec

AMS_PrsTempFlowCal: calibration conditions: P = 1012.5 hPa, T = 15.5 C, flow rate = 1.47 cm^3/sec

AMS_STPConversionFactor: 0.96

AMS_IEOverAB: 5.34E-13

AMS_RIENH4: RIE_{NH4} = 5.4; DMA-sized 300 nm NH_4NO_3 BFSP with concurrently sampled condensation particle counter verification.

AMS_CE: Constant CE=0.5 based on thresholds in Middlebrook et al. (2012). Here, $NH_4/NH_{4,predict}$ = 0.8 (r^2 = 0.96) > 0.75 threshold , ANMF = 0.11 ± 0.15 < 0.4 threshold, relative humidity in the inlet < 80% for 88% of data points (see *InletRH*). Supported by PILS-IC sulfate comparison (m=1.00, r^2=0.88) consistent with other studies (Middlebrook et al., 2012; Takegawa et al., 2005).

AMS_PMCut: $PM_{2.5}$

AMS_InletRH: ambient: inlet RH averages 52 ± 22%; 88% of hourly data points are below 80% RH (inclusive of raining data points with very low aerosol concentration), using Clausius-Clapeyron with ambient temperature, ambient RH, and the mobile lab thermostat setting (15.56 ºC)

AMS_LocalToUTCTime: UTC – 7h

AMS_RelatedInstrumenationInfo: Inside mobile lab held at 15.56 ºC; dedicated inlet.

Other calibrations, etc.: HEPA-filtered ambient air sampled for ~30 minutes every other day (per Aerodyne Research, 2005). PSL size calibration at beginning and end of campaign.

Instrument comparisons: PILS-AMS (17-min resolution): NO_3: m=1.29, r^2=0.76; NH4: m=0.80, r^2=0.50.

Error estimates for the elemental ratios are: O:C (31%), H:C (10%), N:C (22%), and OM/OC (6%) (Aiken et al., 2007).

* Corresponding author. Tel: 1-720-485-9191
E-*mail address*: mishaschurman.ms@gmail.com

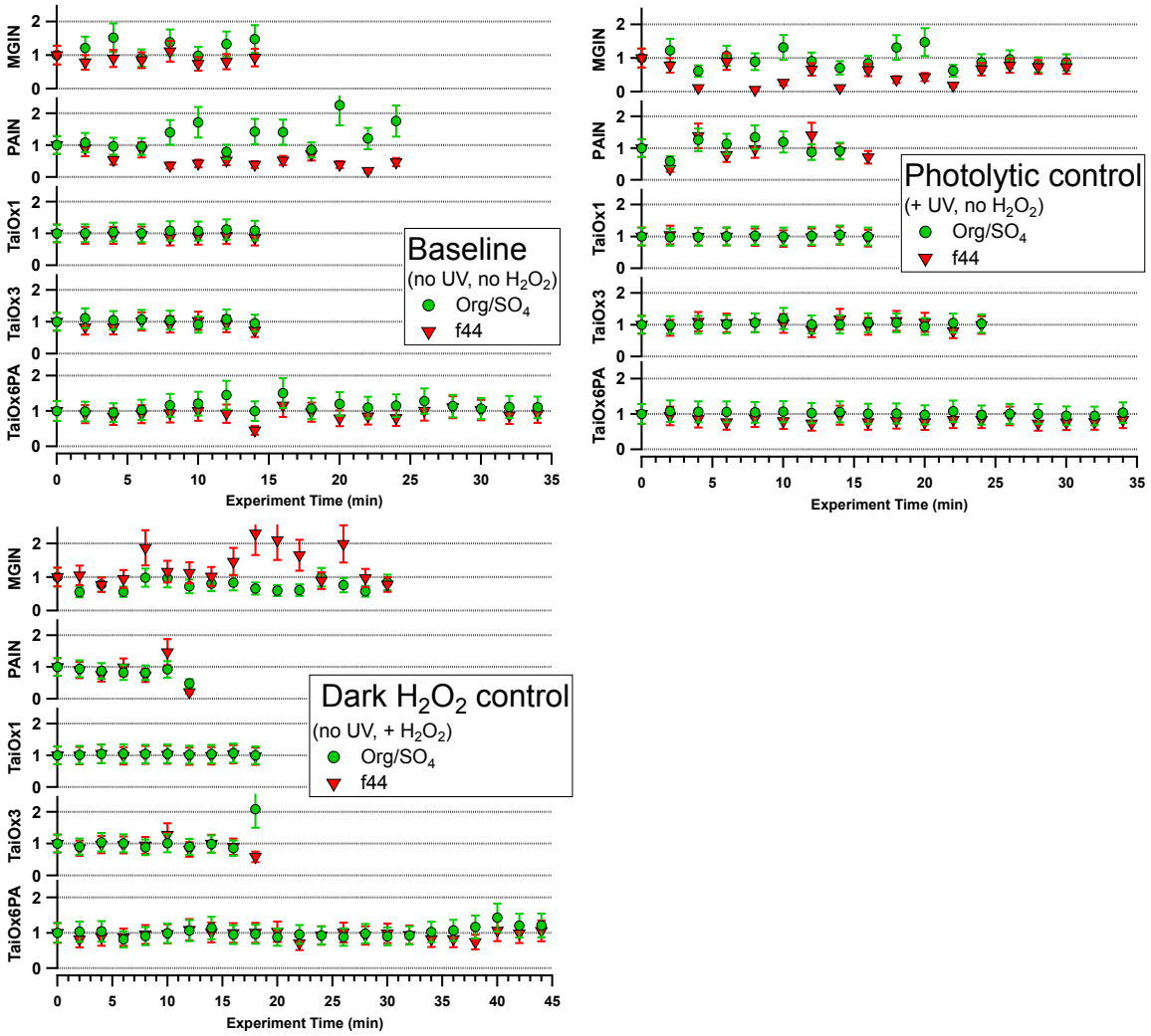

Figure S1: Organics/Sulfate and *f*44 (*mz*44/Organics) normalized to t=0 for dark ('baseline'), photolytic, and hydrogen peroxide control experiments with conditions as noted in the legends; error bars are ± 28% based on propagation of AMS quantification error. Controls for the remaining ambient samples are omitted for brevity. Single-precursor pinonic acid + inorganics (PAIN) and methylglyoxal + inorganics (MGIN) are included for comparison.

S2: Description of variable atomizer output

Variable atomizer output was observed in sporadic single-run (1-min average mass spectrum) mass 'spikes' with no commensurate RH change (Figure S2). The atomizer was draining inconsistently during these 'spikes,' emptying approximately every minute instead of continuously, as observed at the waste container. The spikes may arise from re-entrainment of sample that failed to atomize and collected in the bottom of the chamber, when the waste liquid level rose to the atomizer orifice. Because the atomizer was draining every minute or so, the re-entrained sample might not be significantly different in composition from the current sample, which might explain why composition and mass progress smoothly when normalized to sulfate, as explained in the text and discussed further below. The atomizer was cleaned and re-plumbed a number of times according to manufacturer recommendations for various sample delivery methods; none of these succeeded in rectifying the problem.

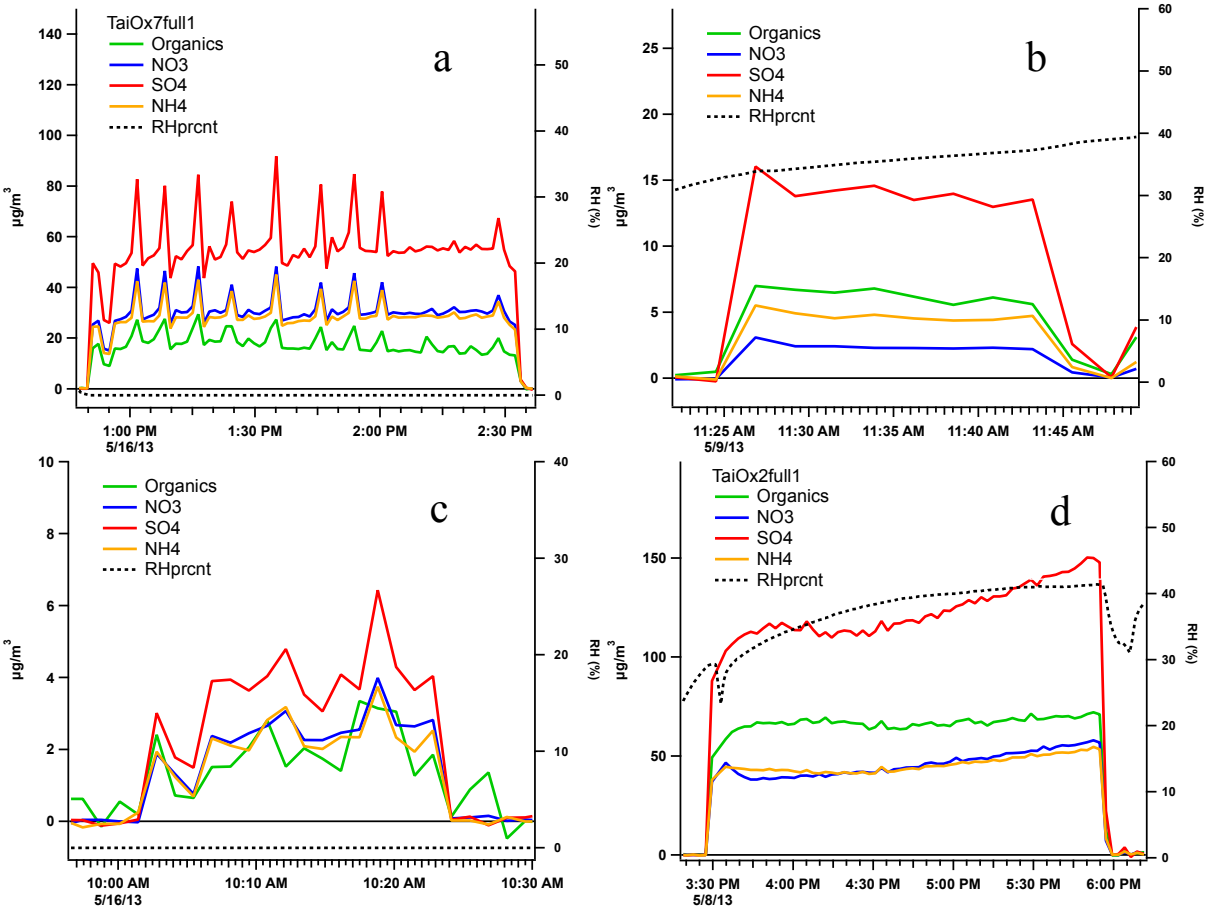

Figure S2: Example experiment timelines showing (a) a full photo-oxidation with mass 'spikes,' (b) a 'baseline' period with increasing RH, (c) a 'baseline' period with steady RH (≈ 0), and (d) a full photo-oxidation with more constant output.

We have observed similar mass 'spikes' in high-RH marine environments when liquid collects on, then is released from, the AMS flow-control orifice; we hypothesize that RH is too low for this to be the case here (see below), and there were none of the pressure and flow fluctuations during spike-affected periods usually caused by AMS orifice blockage.

Some chamber experiments have observed continuous, low magnitude increases in mass output of sulfate correlated with growing sample stream RH (Volkamer et al., 2009); we assume that SO_2 dissolution is a negligible source of sulfate (from laboratory air, for which SO_2 sources are low) and that evaporative loss of volatile S(IV) compounds such as $SO_2 \bullet H_2O$ is not significant, such that if sulfate mass increases during 'baseline' periods (no UV, no H_2O_2) it would necessarily arise from changing atomizer output or particle collection efficiency.

Next, increased RH may enhance water content in oxidized organic particles, which are generally hygroscopic (Kanakidou et al. 2005; Petters & Kreidenweis 2007; Lambe et al. 2011; Jimenez et al. 2009), making them more spherical and increasing collection efficiency by reducing 'bounce' out of the AMS vaporizer; enhancement of collection efficiency by deliquescence when RH exceeds ~80% has been observed (Allan et al. 2004; Matthew et al. 2008). Since these cloud samples originate over a forested mountain in the industrialized North China Plain and approximately 40km from a city of almost 7 million (Jinan, China), a fair amount of oxidized content might be expected and is confirmed in the mass spectra (Figures 4 and S2) in which *m/z* 44 > *m/z* 43 (not shown; the definition of 'low-volatility oxidized organic aerosol,' or LV-OOA). Thus, it is necessary to evaluate whether particle wetting could contribute to fluctuating particle collection efficiency.

RH monitored before the AMS inlet averaged 32.02 ± 13.57% (max. = 66.4%). Since the particles start wet, RH relative to the crystallization point is more relevant to particle water content than deliquescence. Efflorescence RH (ERH) for ammonium-sulfate-α-pinene particles may be very low or eliminated for organic fractions ≥ 0.6, and has been measured at ≤ 30% for lower organic mass fractions (Smith et al., 2012); our organic fractions average 0.42 ± 0.30, so it is likely that between decreased ERH and an RH usually at or above the maximum estimated ERH, our particles did not change phase (i.e. crystallize) and collection efficiency was approximately constant. In any case, increasing RH seemed to have no effect on collected particle mass during baseline periods, as evidenced in panels (b) and (c) of Figure . Installation of a second dryer to combat RH fluctuations reduced RH to near 0% (RH monitor accuracy = 3% at 0-90% RH; see Section 2.3 and Table 2-2 for further information on RH in each experiment). Baseline experiment mass output was not related to RH in either 'humid' or dry conditions.

Sulfate and total mass enhancements have also been observed in cycloalkane ozonolysis experiments under constant RH, where organic particle coatings are thought to increase particle sphericity and therefore collection efficiency (Bahreini et al., 2005); this may contribute to sulfate (and total mass) increases during photo-oxidation experiments, though no sulfate increases were noted during baseline periods as described above. Unfortunately, it is difficult to disentangle SOA formation from possible organic coating effects, if applicable.

Other complications were noted, including very sporadic, abrupt (step-wise) changes in atomizer output unrelated to the mass spikes and unaccompanied by RH changes. It is also possible that liquid water in the sampling lines, observed sporadically at and before the first dryer inlet (when the atomizer did not drain correctly), affects aqSOA quantification in a non-atmospherically relevant fashion by changing partitioning through a) particle/droplet interception or b) gaseous uptake, inducing volatilization from particles; organic coatings might also affect partitioning if they are insoluble, but since most functionalized organics are polar, organic films are usually soluble and seem to have little effect on the partitioning of organics (Donaldson and Vaida, 2006; Kolb et al., 2010). Partitioning effects are difficult to quantify with the current dataset and remain a caveat to the validity of results. Even if partitioning is not affected, it is difficult to distinguish between output inconsistency, altered collection efficiency, and real change in aqSOA production, thwarting direct quantification and necessitating the sulfate normalization described previously.

The AMS is quantitative for nitrate, sulfate, ammonium, chloride, and total organics; because all organic and inorganic sulfur compounds fragment to HSO_x (Farmer et al., 2010), total 'sulfate' signal can be used to normalize component (e.g. organic) mass changes in all samples containing inorganics (i.e. all except PA and MG). See the supplement S4 for further discussion of methodological assumptions and limitations.

S3: Cloud Sample Information

Cloud samples were collected atop Mt. Tai, China, which lies in an industrialized province near metropolitan areas but disallows motorized vehicles locally, using a Caltech Active Strand Cloudwater Collector (CASCC) or a size-fractionating CASCC during the summer of 2008 (Collett et al., 1998; Demoz et al., 1996; Rao and Collett, 1995; Rattigan et al., 2001; Reilly et al., 2001). Sample collection was begun when the cloud liquid water content exceeded 100 mg/m^3, with collection bottles changed every 1-2 hours and samples stored frozen (Shen, 2011); see Schurman (2014) Appendix Section 8.4 for more information on individual samples.

For the ambient samples herein, clouds were present for 0-10 hours (average = 3 ± 4 hrs) preceding collection and the persisted for an average of 6 ± 4 hours after collection, with

only one sample (one of the three mixed to create T1) from a cloud persisting less than the experimental oxidation time of ~2 hours.

Reaction types and naming guide:

Reaction names are a combination of a prefix containing the reaction precursors and suffix containing experiment type (control type, etc.) and replicate number.

Prefixes:

Ambient Cloud: T# (#: 1-7)

Ambient Cloud with added Pinonic Acid: T#PA

Suffixes:

b#: (baseline period) no UV, no H_2O_2; replicate #

ho#: (control) H_2O_2 added, no UV; replicate #

uv#: (control) UV on, no H_2O_2; replicate #

f#: (full photo-oxidation) H_2O_2 added, UV on; replicate #

For example, "T6PAf1" indicates T6 ambient cloud with added pinonic acid precursor, full photo-oxidation, replicate 1.

Table S1: Experimental conditions, name, and concentration of added precursors, if applicable: ammonium nitrate (AN) and ammonium sulfate (AS; always added with AN), and/or pinonic acid (PA) or methylglyoxal (MG). Total Organic Carbon (TOC) is also included. * MGb2 & 4 not included due to instrument malfunction. In the RH column, "-" indicates missing data, and "~0" is at or below the detection limit of the monitor. Multiple values are from replicates of the given experiment (indicated in "Name" column).

Experimental Conditions	Name	PA or MG (uM)	AN&AS (uM)	HOOH (uM)	TOC (mg/L)	RH (%)
(cntrl) PA + inorgs +UV	PAINuv1 & 2	30.00	50	0	3.60	36.33 ±1.25
(cntrl) PA + inorgs + H_2O_2	PAINho1& 2	30.00	50	300	3.60	42.57 ±0.51
(cntrl) PA + inorgs no H_2O_2 no UV	PAINb1, 2, 3, & 4	30.00	50		3.60	-,0,0,0
Tai-Ox 1 no H_2O_2 no UV	Tox1b1	0	0	0	~20	45.11 ±1.61
Tai-Ox 1 + UV	Tox1uv1	0	0	0	~20	51.14 ±0.69
Tai-Ox 1 + H_2O_2	Tox1ho1	0	0	2982.1	~20	53.68 ±0.28
Tai-Ox 1 + UV + H_2O_2	Tox1full1	0	0	3017.4	~20	22.60 ±3.52
Tai-Ox 2 no H_2O_2 no UV	Tox2b1	0	0	0	24.10	27.87 ±2.31
Tai-Ox 2 + UV + H_2O_2	Tox2full1	0	0	3002.7	24.10	38.29 ±2.93
Tai-Ox 3 + UV + H_2O_2	Tox3full1	0	0	292.40	2.86	47.36 ±1.86
Tai-Ox 3 + H_2O_2	Tox3uv1 & 2	0	0	303.57, 300.00	2.86	53.12 ±0.90, 29.67 ±1.94
Tai-Ox 3 + UV	Tox3ho1 & 2	0	0	0	2.86	23.09 ±2.84, 38.61 ±1.31
Tai-Ox 3 no H_2O_2 no UV	Tox3b1				2.86	35.19 ±1.42

Tai-Ox 4 + H_2O_2 + UV	Tox4full1,2, & 3	0	0	301.37, 298.70, 300.83	1.73	33.89± 4.73, ~0,~0
Tai-Ox 4 no H_2O_2 no UV	Tox4b1 & 2	0	0	0.00	1.73	21.79± 1.15, 0
T6 + PA no H_2O_2 no UV	Tox6PAb1	30.00	0	0	9.15	~0
T 6 + PA +UV	Tox6PAuv1	30.30	0	0	9.15	~0
T 6 + PA + H_2O_2	Tox6PAho1	30.36	0	303.57	9.15	~0
T 6 + PA +UV+ H_2O_2	Tox6PA1	30.49	0	304.88	9.15	~0
T 7+PA no H_2O_2 no UV	Tox7PAb1	30.49	0	0	10.06	~0
T 7+ PA +UV+ H_2O_2	Tox7PA1	30.49	0	304.88	10.06	~0
(cntrl) MG + inorgs no H_2O_2 no UV	MGINb1 & 2	60	50	0	2.16	~0
(cntrl) MG + inorgs + UV	MGINuv1	60	50	0	2.16	~0
(cntrl) MG + inorgs + H_2O_2	MGINho1	60	50	300	2.16	~0
Tai-Ox 7 no H_2O_2 no UV	Tox7b1	0	0	0	6.40	~0
Tai-Ox 7 + UV + H_2O_2	Tox7full1	0	0	297.52	6.40	~0
Tai-Ox 7 + UV	Tox7uv1	0	0	0	6.40	~0
Tai-Ox 7 + H_2O_2	Tox7ho1	0	0	300	6.40	~0

Table S2: Analysis of each cloud water sample used herein, discussed in depth in Shen et al. (2011). The 'Collector' column refers to type of collector used, where C = CASCC, L = size-fractionated CASCC, large droplets (D_p>~16μm), S = size-fractionated CASCC, small droplets (~4μm < D_p < ~16μm).

Exp. #	**Sample**	**pH**	**Cl**	**NO2**	**NO3**	**SO4**	**Na**	**NH4**	**K**
			μN	μN	μN	μN	μN	μN	μN
T1	TC062508A01	6.61	123.	24.0	876.	4060	43.4	4300	138.
T1	TC070308A03	5.38	51.4	12.3	343.	1810	22.1	2360	37.9
T1	TS061908A01	4.47	143.	10.4	1200	2310	20.7	3590	172.
T2	TS061808A03	3.32	154.	4.36	970.	1720	14.3	1790	115.
T3	TL070408A09	6.37	12.5	2.41	52.2	271.	7.48	257.	9.39
T4	TC070408A13	4.74	7.45		63.6	202.	1.58	200.	2.60
T6	TC071408A01	3.70	48.9	2.14	336.	1130	10.7	1130	13.61
T7	TC070808A11	4.58	40.8	2.34	376.	885.	8.82	1034.	47.5
Exp. #	**Sample**	**Mg**	**Ca**	**TC**	**TN**	**TIC**	**TOC**	**H2O2**	**HCHO**
		μN	μN	ppm	ppm	ppm	ppm	μM	μM
T1	TC062508A01	26.5	465.	29.9	92.7	9.34	20.5	6.75	8.17
T1	TC070308A03	17.7	178.	28.1	51.7	10.5	17.5	79.8	5.82
T1	TS061908A01	16.2	109.	24.2	84.5	2.59	21.6	0.96	8.20
T2	TS061808A03	6.81	34.7	30.7	48.9	6.60	24.1	1.92	27.5
T3	TL070408A09		11.6	4.74	6.36	1.88	2.86	94.4	3.39
T4	TC070408A13		8.11	2.50	5.26	0.78	1.73	9.42	2.16
T6	TC071408A01	22.8	101.	7.53	28.4	1.98	5.55	50.5	11.1
T7	TC070808A11	8.08	79.2	8.75	28.1	2.35	6.40	29.7	21.3
Exp. #	**Sample**	**S4**	**Fe**	**Mn**	**Start Time**		**End Time**		**Collector**
		μM	μg/L	μg/L					
T1	TC062508A01	26.0	953.	76.1	6/25/2008 23:10		7/3/2008 0:00		C

T1	TC070308A03	108.	373.	101.	7/3/2008 23:00	7/3/2008 0:00	C
T1	TS061908A01	52.3	632.	39.7	6/19/2008 19:00	6/19/2008 21:00	S
T2	TS061808A03	31.3	849.	22.5	6/19/2008 0:00	6/19/2008 1:00	S
T3	TL070408A09	20.6	44.6	18.6	7/5/2008 10:00	7/5/2008 12:00	L
T4	TC070408A13	15.2	710.	6.53	7/5/2008 17:00	7/5/2008 18:00	C
T6	TC071408A01	30.6	384.	29.3	7/14/2008 18:00	7/14/2008 19:00	C
T7	TC070808A11	9.85	206.	17.1	7/9/2008 0:30	7/9/2008 1:30	C

S4: Methodological Assumptions and Limitations

Sulfur Normalization:

Sulfur normalization assumes that sulfur partitioning during drying is constant and SO_2 dissolution from room air is negligible, assumptions that are supported by constant 'CS' and HSO_x-family fragment mass between experiment beginning and end.

Equivalent OH Exposures:

As outlined in Section 2.3, the 'equivalent ageing times' (i.e. OH exposures) that lead to organic mass loss must be compared to the real atmosphere. The $[OH]_{aq}$ herein is similar to that in ambient cloud water. We use $[OH] \approx 10^{-14}$ M (in total from both added H_2O_2 and that present in the ambient sample); cloud estimates = 10^{-14}– 10^{-12} M (Arakaki and Faust, 1998; Ervens et al., 2003a). We assume that ageing time in these experiments is directly equivalent to ambient ageing time, at least in terms of OH, which is often the dominant aqueous oxidant, though organic radicals may also be produced through photolysis and/or OH reaction. Neither organic mass nor oxidation indicator *f*44 change significantly under UV-only or H_2O_2-only control conditions, indicating that neither Fenton reactions nor hydrogen peroxide-initiated reactions produced significant amounts of aqSOA (see Section 2.3) and, hence, that aqSOA formation in the full photo-oxidation arises from OH-initiated reactions. We also must assume that concentrations and forms of radical-producing organics did not change significantly during sample storage and that differences in irradiation between our UV source and the sun are small.

S5: Quantifying Formic Acid via AMS

'Formic acid' ($CH_2O_2^+$ @ *m/z* 46) receives special attention here for its volatility and impact on organic mass retention; upon collection, the cloud samples contained formic acid in some quantity (Shen, 2011). Though other molecules may fragment to $CH_2O_2^+$ and the complexity of the ambient matrix prevents determination of $CH_2O_2^+$ contribution from specific parent molecules, we move forward using $CH_2O_2^+$ signal to represent an upper bound on 'formic acid' production. Note that some studies exclude $CH_2O_2^+$ for its proximity to and therefore possible interference from NO_2^+ (Zhang et al. 2005; Duplissy et al. 2011); it is included here following the standard half-max, half-width fitting rule, but it is notable that 'formic acid' is weakly correlated to total nitrate in T1 and T3 ($r^2 \approx 0.7$), the only runs for which we see significant formic acid formation. Both organic and inorganic nitrogen fragments (CHON and CHN, NO_n) increase in some experiments, possibly from formation of less-volatile organic nitrogen products as discussed later. However, the presence of nitrate in the runs with no formic acid (and little change in fitting residuals over the course of all experiments) suggests that the 'formic acid' is not a fitting error and that correlations between formic acid and nitrate may arise from real co-increases. Note that a given fragment, such as formic acid, may come from multiple parents; this analysis explores organic composition change *qualitatively* through functional group fragments, but cannot be used to quantify product formation in such a complex mixture.

S6: Delta Analysis and High Molecular Weight Compounds

Higher molecular weight compounds were detected, many of which are important in their mass bins (and without influence of a larger coincident peak), suggest highly functionalized molecules and/or oligomer formation, and are explored below; however, most of these fragments are too low in total mass to construct meaningful normalized timelines and so will be presented using important fragment series expressed through delta patterns. Some of these molecules are listed in Table S3 along with tentative identification from other studies in which they have been observed.

Important fragment series can expressed through delta patterns, which rely on the tendency of organic molecules to lose CH_2 groups sequentially during fragmentation such that the resulting signal peaks are separated by 14 atomic mass units (amu); functional group composition dictates the *m/z* values of the peaks such that delta (Δ) = $m/z - 14n + 1$, where n is the number of methylene (CH_2) bridges on the functional group (Table S2, McLafferty and Turecek, 1993). Clear delta shifts toward positive values at the end of the T1 and T3 experiments (also T4 and T7), indicating the predominance of functionalized organics (Figure S2). Decreases are most notable at Δ_0 (alkenes, cycloalkanes), Δ_{-2} (dienes, alkynes), Δ_{-4} (terpenes, phthalates), and Δ_{-6} (phenyl alkyls, etc.); the greatest enhancements are seen in Δ_1, which generally contains cycloalkyl/alkanones, diketones, and unsaturated esters, and Δ_3, representing aldehydes, cycloalkanols, etc., with small decreases in Δ_2 (alkyls, saturated carbonyl; not significant for T1).

A number of studies suggest that the dominant peak structure is driven by aerosol source type and can be illustrated through delta values, where positive Δ indicates (usually aged) anthropogenic sources and negative Δ suggests (especially, fresh) biogenic sources (Bahreini et al., 2005; Canagaratna et al., 2007; Kiendler-Scharr et al., 2009). Δ values of 0, 2, and 3 may suggest aged anthropogenic sources and have been observed during urban ambient studies (Drewnick et al., 2004; Schneider et al., 2004).

Table S3: Summary of delta values indicated fragments and/or functional groups, adapted from McLafferty & Turecek (1993).

Delta	Indicated Functional Groups	Delta	Indicated Functional Groups
-7	Phenyls	0	Alkenes, Cycloalkanes, Alkyl cyanides
-6	Phenylalkyls, Benzoyls, ROCOOR-species, Chloroalkyls	1	Alkenes, Cycloalkyl, Diketones, Unsaturated esters, Cyclic amines
-5	R-phenyls, Aminoaromatics	2	Alkyls, Saturated carbonyl
-4	Terpenes and derivatives, Phthalates	3	Aldehydes, Cycloalkanols, Alkyl amines, Amides, Nitrites
-3	R-phenyls, Cycloalkenes	4	Alcohols, Acids, Esters, ROCO-R`-CO
-2	Alkynes, Cycloalkenes, Unsaturated/cyclic w/ O: alcohol, ether	5	Cyclic sulfides, Nitrates, ROCOCHR`, CR_2ONO
-1	Ketones (unsaturated), Alkyl cyanides, Retro-Diels-Alder product (cyclohexene)	6	Unsaturated aryls, Alcohols, RCOOR`-rearrangments, Sulfides

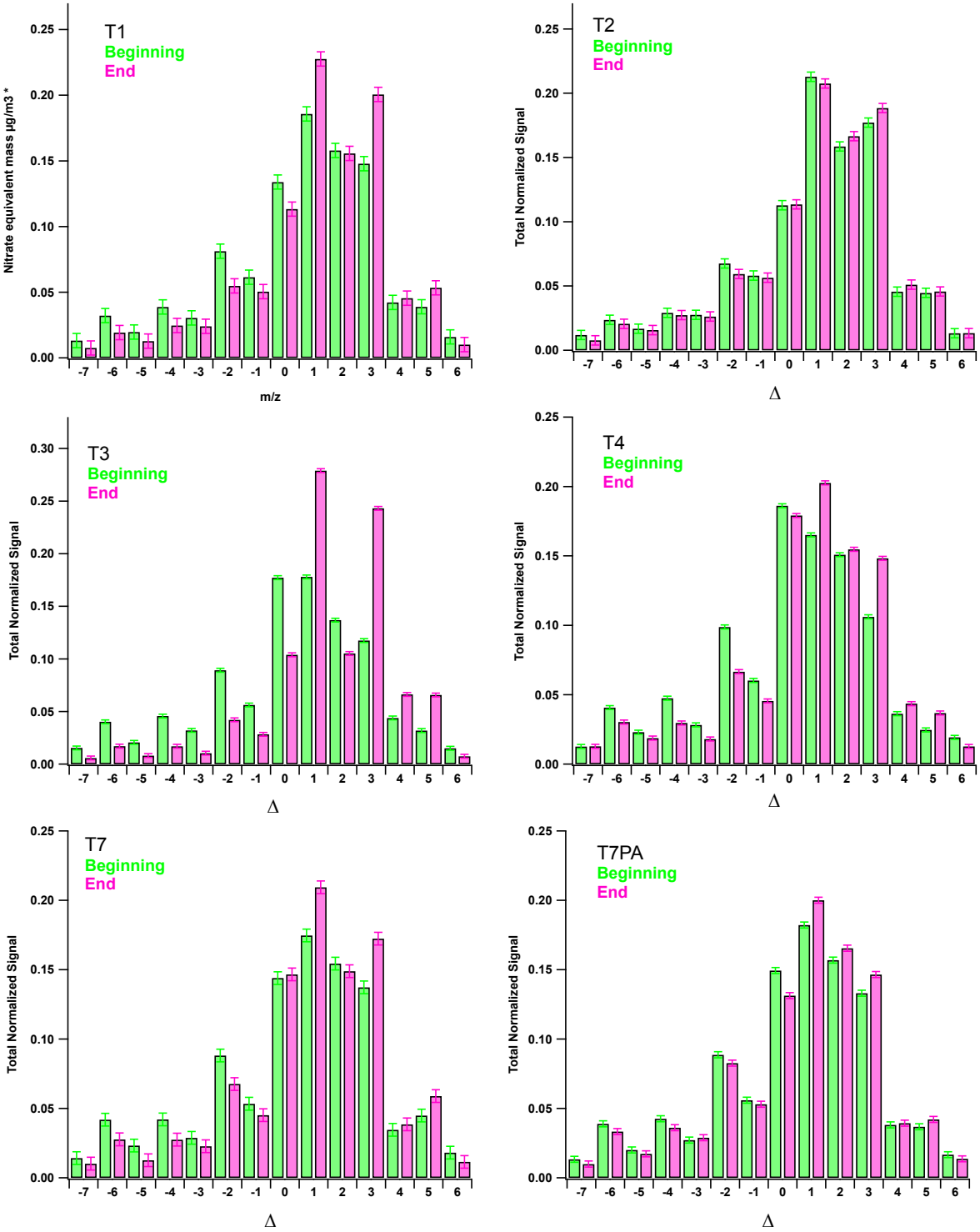

Figure S3: Total normalized signal in fragments with the given delta (Δ) value in the 5-minute average experiment beginning or end total organic mass spectrum. Error bars are the normalized average signal error over all mass bins for the given experiment.

Difference Spectra

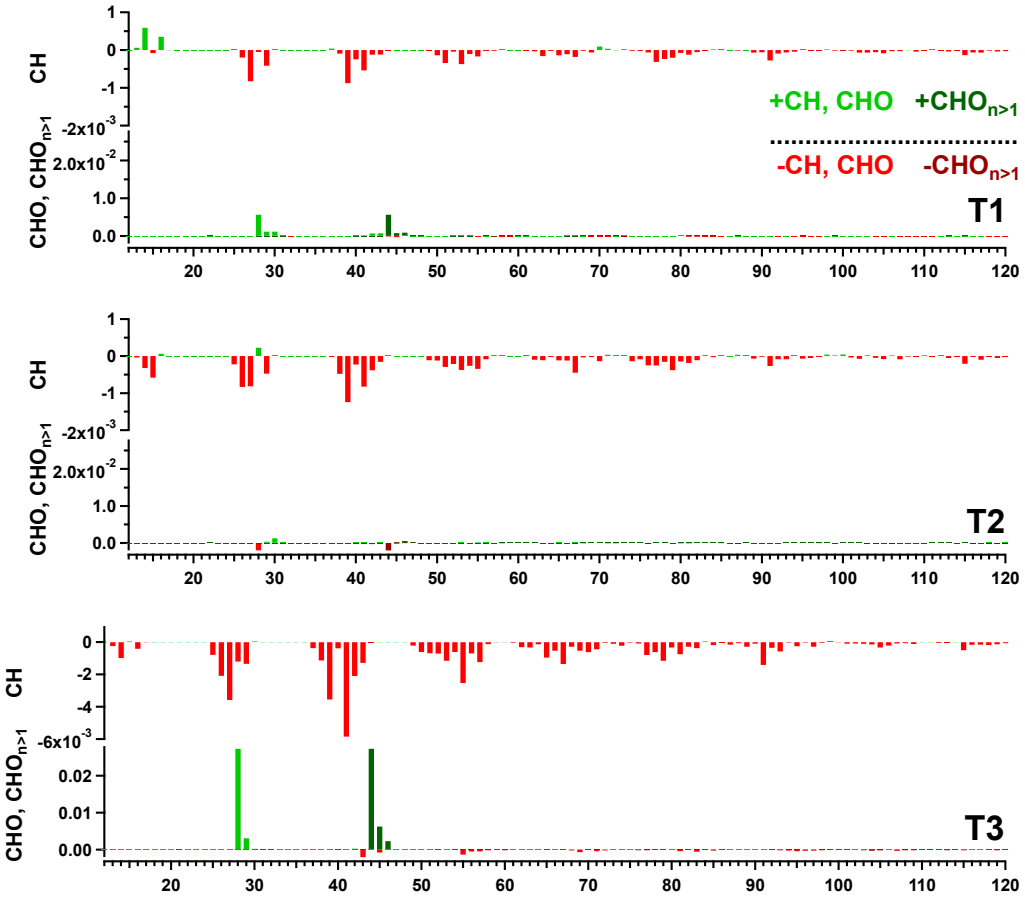

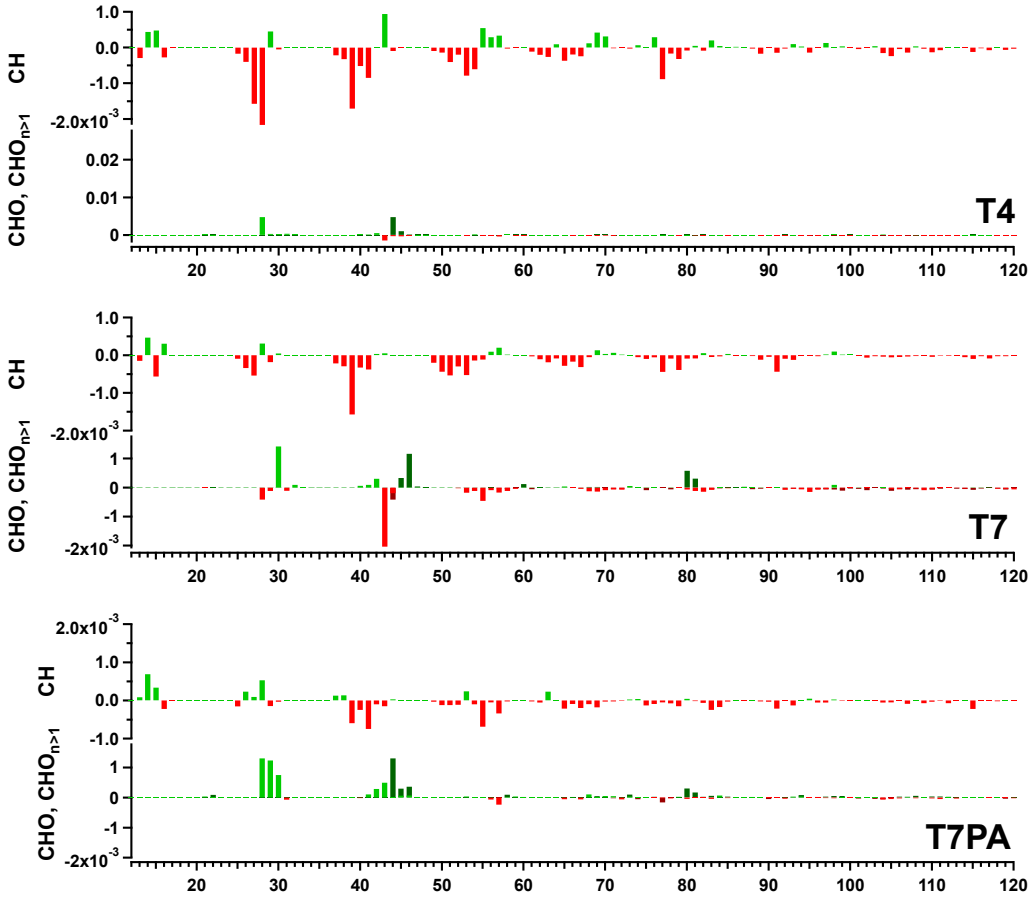

Figure S4: Ambient-sample fragment-family difference mass spectra, subtracting the normalized 5-minute average spectrum from t=0 from that at the experiment's end.